VER
Vascular & Endovascular Review

Cost-Effective and Transparent Diagnosis of COVID-19 and Pneumonia using X-ray Images: A Machine Learning Approach

Sujata Ghatak[1], Mousmi Gupta[2], and Satyajit Charabarti[3]

[1]Computer Applications, Assistant Professor, University of Engineering and Management, Kolkata, India
[2]Research Lead, Asian Development Research Institute (ADRI), Patna
[3]Computer Science and Engineering, Professor, Institute of Engineering and Management, Kolkata, India Email: Sujata.Ghatak@uem.edu.in; mousumi.gupta@adriindia.org; satyajit.chakrabarti@iem.edu.in
***Corresponding author**

ABSTRACT

The demand for rapid, cost-effective, and precise diagnostic instruments for chest-related conditions, including COVID-19 and pneumonia, has become more pressing in the aftermath of the COVID-19 pandemic. Despite the remarkable results that deep learning-based approaches have achieved, they frequently necessitate large annotated datasets, substantial computational resources, and a lack of interpretability. In contrast, this study suggests a low-cost hybrid machine learning-based diagnostic framework that classifies cases into three categories: Normal, Pneumonia, and COVID-19, based on interpretable features extracted from chest X-ray images. In order to quantify structural complexity, texture variability, and edge information, three critical features—Fractal Dimension, Entropy, and Edge Density—were extracted from each image. The statistical analysis of ANOVA confirmed that all three features exhibited significant variation among the three classes ($p < 0.005$). This was further substantiated by the visual separability demonstrated by boxplots. The machine learning classifier was trained using the extracted features, resulting in an overall accuracy of 77.13 percent. The model was notably effective in distinguishing between Pneumonia (F1- score: 0.84) and Normal (F1-score: 0.64). However, the classification of COVID-19 (F1-score: 0.53) exhibited some overlap with Pneumonia. The ROC curves demonstrated a robust discriminative capacity, with AUC values of 0.87 for Normal, 0.84 for COVID-19, and 0.82 for Pneumonia. This method is interpretable and lightweight, and it offers a cost- effective solution for the preliminary diagnosis of pulmonary disease. Additionally, it establishes a solid foundation for future improvements that will incorporate more complex features and models.

KEYWORDS: Pnemonia, Machine learning, Fractal dimension, entropy, Covid-19

How to Cite: Sujata Ghatak, Mousmi Gupta, and Satyajit Charabarti., (2025) Cost-Effective and Transparent Diagnosis of COVID-19 and Pneumonia using X-ray Images: A Machine Learning Approach, Vascular and Endovascular Review, Vol.8, No.18s, 120-127

INTRODUCTION

The global COVID-19 epidemic has made it even more important to have quick, reliable, and cheap diagnostic techniques for respiratory disorders. Chest X-ray (CXR) imaging is now an important tool for initial screening and illness surveillance because it is widely available and inexpensive. However, interpreting CXRs by hand can take a long time, be subjective, and differ from one radiologist to the next. This has made more people interested in computer-aided diagnostic (CAD) systems to help doctors make decisions.

The automatic classification of medical images with high accuracy has been made possible by recent advancements in deep learning. However, these methods frequently necessitate substantial computational capacity, large volumes of annotated data, and frequently a lack of interpretability—a critical requirement for healthcare applications. Additionally, black-box models may present obstacles to clinical adoption, particularly in environments where transparency and explainability are essential.

In order to overcome these constraints, we suggest a hybrid machine learning-based diagnostic pipeline that prioritises interpretability, simplicity, and minimal computational cost. Our approach employs handcrafted statistical and structural features that are computationally efficient and straightforward to interpret, rather than complex deep neural networks. In particular, we extract three critical features from chest X-rays: Fractal Dimension (FD) to characterise spatial texture and transitions, Shannon Entropy to reflect image randomness or information content, and Edge Density to capture structural complexity. Conventional machine learning classifiers, including logistic regression and decision trees, are trained using these features, which are statistically analysed for their discriminative power.

The objective of this investigation is to illustrate that a combination of classical machine learning algorithms and interpretable, biologically pertinent features can produce reliable diagnostic performance for the differentiation of Normal, COVID-19, and Pneumonia cases. The framework that has been proposed is particularly well- suited for resource-constrained environments where the deployment of large-scale AI systems is not feasible and where decision support must be both rapid and comprehensible.

LITERATURE REVIEW

The use of chest X-ray imaging for COVID-19 and pneumonia detection has garnered significant research interest, exploring a spectrum of approaches from lightweight models to fractal-based descriptors and explainable AI.

1.Lightweight and Ensemble Deep Learning Systems Siddiqi Javaid [1] introduced CovidLite, a compact CNN tailored for COVID-19 detection with minimal computational complexity. Similarly, Ali et al. [2] developed an ensemble of CNNs to enhance diagnosis robustness and manage class imbalance. Tur [7] proposed lightweight ensemble networks suitable for resource- limited settings. Subashini et al.[8] applied transfer learning ensembles to ensure cross-disease generalizability.
2.Hybrid and Explainable Models Incorporating Fractal Features
Hamal et al.[5] combined fractal dimension analysis with CNN features, demonstrating structural complexity provides complementary information to deep networks. Chakraborty et al.[4] emphasized the value of combining socio-clinical factors with imaging via multivariate fuzzy clustering. While Tamal et al. [3] integrated fuzzy logic with CNNs to increase interpretability in severity assessment, Arias-Londoño et al. [6] focused on interpretable multi-modal ML for respiratory disease detection.
3.Interpretability and Feature-Based Classical ML Habib Rahman [10] and Iqbal et al. [11] developed interpretable, feature-driven models (e.g., texture and statistical descriptors) for COVID-19 and tuberculosis classification using chest X-rays. Xue et al. [12] leveraged texture and fractal descriptors in a non-deep ML framework to classify lung disease patterns efficiently.
4.Multimodal and Transfer Learning Enhancements Alahmari et al.[9] introduced a multimodal explainable system, integrating cough audio and X-ray data with human-understandable models . Ayyachamy[17] designed transfer-learning workflows tailored to COVID-19 detection from chest X-rays. Kumar Bhowmik [18] optimized CNN architectures for improved speed and efficiency in CXR classification. Kibria et al. [19] used ensemble deep models with interpretability overlays for reliable COVID-19 detection. Pal et al. [13] and Liu et al. [20] contributed frameworks emphasizing transparency and generalization using interpretable features.\

In summary, the existing literature reveals a growing emphasis on lightweight, accurate and explainable models for chest X-ray–based diagnosis of respiratory diseases. While deep learning and ensemble models achieve high accuracy, they often lack interpretability. Conversely, classical machine learning pipelines that rely on handcrafted features—including fractal dimension, entropy, and edge density—offer transparency but may compromise on performance. Our work bridges this gap by combining statistically validated handcrafted features with efficient machine learning classifiers, offering a low-cost, interpretable, and robust diagnostic framework suitable for resource-constrained clinical settings.

MATERIALS AND METHODS

This study proposes a low-cost hybrid diagnostic model for classifying chest X-ray images into three categories: Normal, pneumonia, and COVID-19. The detailed flow chart has been provided in Fig 1A. The methodology integrates fractal analysis, statistical features, and traditional machine learning to achieve an interpretable and effective classification. The major steps of the proposed methodology are described in the following.

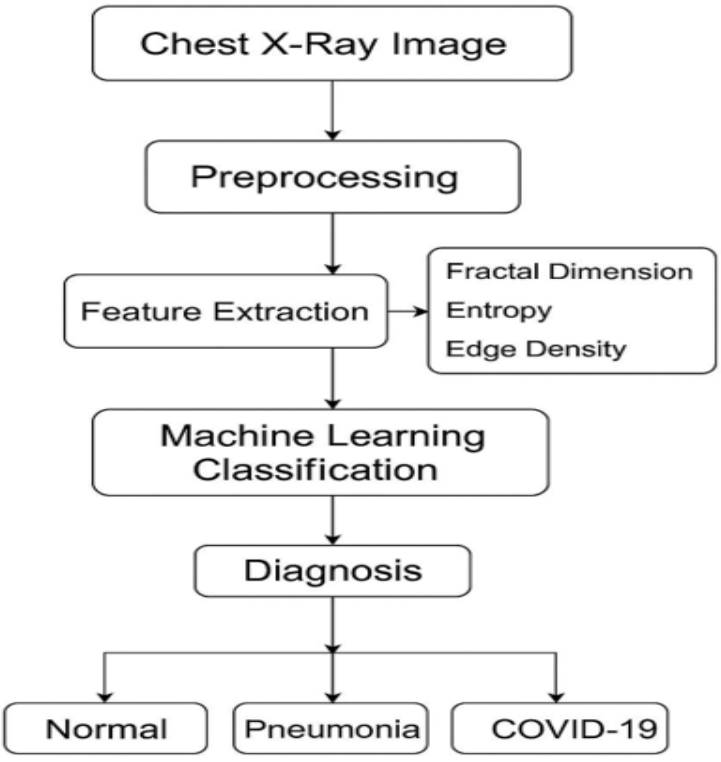

Fig 1A: Flow chart of the diagnosis of X-Ray images using Machine Learning approach.

A. Image Acquisition and Preprocessing

A chest X-ray image I serves as the system's input. Subsequent pre-processing operations are implemented to ensure the accuracy and quality of the input data.

- The image I is transformed into greyscale, if it is not already in that format.
- The greyscale image is scaled to a standardized resolution of 256 × 256 pixels.
- In order to emphasise anatomical details and improve contrast, histogram equalisation is implemented.

- A global thresholding technique, such as Otsu's method, is employed to transform the greyscale image into a binary image B.

B. Fractal Dimension Estimation using Box Counting Method

The box-counting method is employed to estimate the Fractal Dimension (FD). The complexity of structures within the binary image B is quantified in this phase.

1. Choose a predetermined assortment of box sizes $S = \{s1, s2, \ldots sn\}$
2. For each box size $si \in S$
- Partition the binary image B into non- overlapping boxes with specified dimensions $si \times si$.
- Determine the quantity of boxes N(si) that encompass a minimum of one foreground pixel.
3. For each log(N (si)) versus log(1/(si)) for all values of (si).
4. Estimate the slope of the fitted line by performing linear regression. The fractal dimension D is determined by the negative of this inclination.

C. Feature Extraction

Two more features are extracted to augment the model's discriminating power:

- Shannon Entropy (E): Assesses the unpredictability or informational content of the greyscale image. It is characterised as:

$$E = -\sum_{i=0}^{255} pi \log 2\ pi$$

where pi represents the normalized histogram value of pixel intensity i.

- Edge Density (ED): Reflects the structural variance within the image. It is computed as:

1. To get an edge map, use an edge recognition filter, such as the Sobel operator.
2. Enumerate the edge pixels above a threshold T .
3. Compute

$$ED = \frac{No\ of\ Edge\ Pixels}{Total\ No\ of\ Pixels}$$

The conclusive feature vector for each image is delineated as:

$F = [D, E, ED]$

D. Classification using Machine Learning

A classic, inexpensive, interpretable classifier like Decision Tree, Support Vector Machine (SVM), or k- Nearest Neighbors (k-NN) is given the retrieved feature vector F. A dataset of chest X-rays that have been labelled

as Normal, Pneumonia, or COVID-19 is used to train the classifier.

Here are the steps involved in the categorization process:

- Training Phase:
1. Divide the dataset into training and test sets.
2. Utilize the feature vectors F together with their associated class labels to train the classifier.
- Testing/Inference Phase:
3. Utilize the identical preprocessing approach to extract characteristics from novel chest X-ray images.
4. Utilize the trained classifier to predict the class label.

E. Evaluation Metrics

The classifier's performance is assessed using conventional measures.

- Accuracy
- Precision
- Recall
- F1-Score
- Confusion Matrix

Cross-validation, such as 5-fold or 10-fold, can be utilized to evaluate generalizability and reduce overfitting.

F. Datasets Used

The “Chest X-ray (COVID-19 & Pneumonia)” dataset by
\cite{29} comprises 6,432 chest X-ray images classified into three categories: COVID-19, Pneumonia, and Normal (healthy). The photos are categorised into training and testing directories, each comprising distinct subfolders for the three classes, rendering them appropriate for immediate application in machine learning and deep learning processes. This dataset is designed for the construction and assessment of diagnostic models that categorise COVID-19 cases in comparison to other pneumonia infections and healthy individuals. It functions as a significant resource for medical picture analysis, AI- driven diagnostics, and educational applications. Nevertheless, it lacks supplementary material, including patient demographics and imaging conditions, rendering it more appropriate for image-based classification tasks than for comprehensive clinical research.

This technology offers an efficient, interpretable, and economical diagnostic pipeline by utilising fractal geometry, statistical image analysis, and conventional classifiers. It circumvents the computational intricacies of deep learning or fuzzy systems while preserving robust performance, rendering it suitable for implementation in resource-constrained environments.

RESULT AND DISCUSSION

This study's feature-based analysis offers significant insights into the possible application of statistical descriptors—specifically fractal dimension, entropy, and edge density—to distinguish between Normal, Pneumonia, and COVID-19 cases in chest X-ray images. This discourse elucidates the interpretability and discriminatory power of each feature, as well as the correlations identified among them, employing diverse visualization and statistical methodologies.

The fractal dimension, which quantifies geometric complexity or self-similarity in image patterns, exhibits significant potential in differentiating normal from pathological situations (i.e., pneumonia and COVID-19) [21,22]. The pair plot and corresponding distribution curves indicate that both the COVID and Pneumonia classes display elevated fractal dimension values concentrated between around 1.7 and 2.0. Conversely, the Normal class exhibits a more condensed distribution with comparatively lower fractal dimension values, indicating reduced structural irregularity in healthy lung tissue. This signifies that fractal complexity escalates in infected lungs as a result of textural disturbances. The resemblance in distributions between COVID and Pneumonia suggests that, although fractal dimension is proficient in identifying Normal instances, it may not be adequate by itself to consistently differentiate between the two illnesses. This constraint highlights the need for utilising fuzzy logic or non-linear decision limits to attain greater classification precision.

Moving to entropy, which quantifies the randomness or information content in an image, the classes display overlapping yet distinguishable characteristics [23,24,25]. COVID cases are marked by a broader spread in entropy values, signifying more diverse texture complexity possibly due to heterogeneous lesion appearances. Normal cases cluster around moderate entropy values, reflecting the relative uniformity of healthy lung tissue. Pneumonia shares some overlap with both classes but tends to lean toward COVID in terms of variability. Although entropy alone may not provide sharp decision boundaries, it augments class separability when combined with fractal dimension. This synergy suggests the presence of complementary information carried by the two features, reinforcing the argument for multivariate modeling over single-feature reliance.

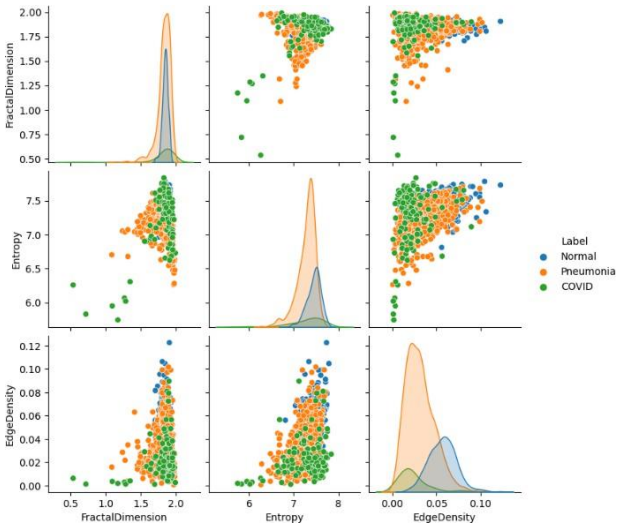

Fig. 1. Pairplot diagram of extracted features (Fractal Dimension, Entropy, and Edge Density) across the three classes: Normal, Pneumonia, and COVID-19.

Edge density, calculated by methods such as Canny edge detection, reveals an additional aspect of differentiation [26,27,28]. The investigation indicates that Normal cases have greater edge density, presumably owing to the distinct delineation of anatomical components in healthy lungs. Conversely, COVID examples exhibit a closely grouped low edge density, likely due to extensive opacification obscuring distinct edge borders. Pneumonia cases are generally situated between extremes, however in certain instances, they tend to align more closely with the Normal range. This stratification pattern indicates that edge density is very proficient in distinguishing COVID instances from Normal cases. The distinct separation between these classes in the distribution plot suggests that edge density, in conjunction with fractal dimension and entropy, can enhance the robustness of classification

systems.

The pairwise scatter plots presented in Fig. 1 reinforce these conclusions by illustrating the interactions of attributes across classes. In the Fractal Dimension against Edge Density plot, COVID instances are clearly situated in regions of high fractal dimension and low edge density, while Normal cases are found in areas of medium-to-high edge density with marginally lower fractal dimension values. Pneumonia intersects with both categories, signifying its intermediate characteristic behaviour. This plot is particularly effective for delineating linear or non- linear decision boundaries that can distinguish COVID from Normal, despite some residual uncertainty between COVID and Pneumonia. The Entropy vs Fractal Dimension scatter plot exhibits class-specific diagonal trend lines, indicating distinct patterns of structural complexity and textural information for each illness category.

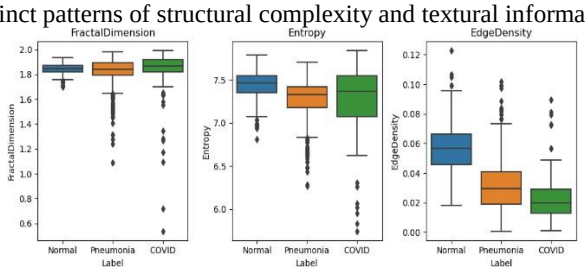

Fig. 2. Box plot diagram of extracted features (Fractal Dimension, Entropy, and Edge Density) across Normal, Pneumonia, and COVID-19 classes.

Fig. 3 presents a correlation matrix that elucidates the interrelationship among the three derived features: Fractal Dimension, Entropy, and Edge Density. The heatmap demonstrates that Fractal Dimension exhibits minimal correlations with both Entropy (0.18) and Edge Density (0.13), indicating that it reflects distinct structural or geometric complexity in chest X-ray images, largely independent of texture randomness or edge characteristics. The independence of fractal dimension renders it a particularly valuable attribute, as it provides non- redundant information to the classification model

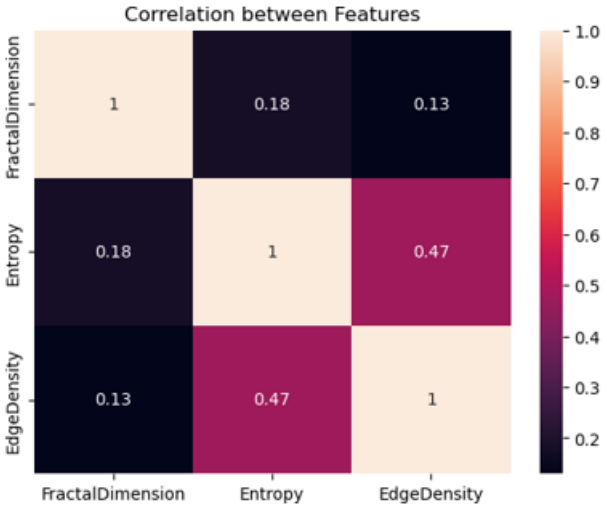

Fig. 3. Correlation heatmap of extracted features (Fractal Dimension, Entropy, and Edge Density)

Conversely, Entropy and Edge Density demonstrate a moderate positive correlation of 0.47, suggesting a degree of shared information between these two metrics. This may result from places exhibiting more texture complexity (higher entropy) frequently generating more edges during edge detection, particularly in instances such as Pneumonia when uneven textures are evident.

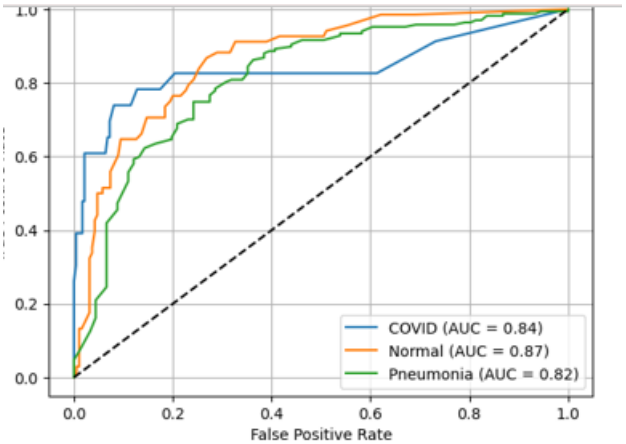

Fig. 4. Receiver Operating Characteristic (ROC) curves for the multi- class classification task (Normal, Pneumonia,

COVID-19).

The low to moderate correlation scores indicate that all three aspects provide complementary insights into the X- ray data. The minimal redundancy among these features bolsters the argument for their utilisation in a multi-feature classification framework, wherein each feature contributes a unique layer of discriminatory power, resulting in a more robust and generalisable diagnostic model for differentiating between Normal, Pneumonia, and COVID- 19 chest X-ray images.

The ANOVA (Analysis of Variance) results offer a statistical basis for evaluating whether the mean values of the retrieved features—Fractal Dimension, Entropy, and Edge Density—significantly differ across the three diagnostic categories: Normal, Pneumonia, and COVID- 19.

The ANOVA test for Fractal Dimension produces an F- statistic of 5.4524 and a p-value of 0.0044. This signifies a statistically significant difference across the groups at the 0.01 level, however with a reduced F-statistic relative to the other features. This outcome substantiates that fractal complexity differs between illness states, especially between normal and pathological categories, while COVID and pneumonia may display some overlap. Detailed ANOVA analysis is shown in below

ANOVA Results ---
FractalDimension: F-statistic = 5.4524, p-value = 0.0044
Entropy: F-statistic = 65.2953, p-value = 0.0000 EdgeDensity: F-statistic = 326.8575, p-value = 0.0000

Entropy demonstrates a far greater distinction, evidenced by an F-statistic of 65.2953 and a p-value nearing zero. The pronounced statistical significance indicates that the textural randomisation of chest X-rays is markedly different among the three categories. COVID instances exhibit greater entropy values, but Normal and Pneumonia cases are more closely clustered yet remain distinct—underscoring entropy's efficacy as a discriminator, particularly when combined with additional variables.

The most significant group differentiation is shown in Edge Density, with an F-statistic of 326.8575 and an almost negligible p-value. This outcome illustrates that edge-based information varies significantly among the classes. Conventional views often possess the greatest edge density owing to enhanced visibility of lung structures, whereas COVID images demonstrate markedly less edge density. Pneumonia images are generally positioned between categories, frequently resembling Normal in certain instances.
These statistical findings are further visually confirmed through boxplots shown in Fig. 2, which clearly show non- overlapping or minimally overlapping interquartile ranges, especially for Edge Density and Entropy. The boxplots provide intuitive visual evidence that aligns well with the ANOVA statistics—supporting the conclusion that the extracted features are statistically significant and visually separable across the diagnostic categories. This dual evidence—statistical and visual—strengthens the credibility of using these features in a diagnostic pipeline, either individually or in combination, for effective discrimination of chest X-ray patterns related to COVID- 19 and Pneumonia.

Table 1: Presents The Precision, Recall, F1-Score, And Support Values For Each Class (Covid, Normal, And Pneumonia) Obtained From The Machine Learning Classification Model.

Class	Precision	Recall	F1-Score	Support
COVID	0.67	0.43	0.53	23
Normal	0.72	0.57	0.64	68
Pneumonia	0.79	0.9	0.84	167
Accuracy			**0.77**	258
Macro Avg	0.73	0.64	0.67	258
Weighted Avg	0.76	0.77	0.76	258

Table :2 Presents The Distribution Of Correctly And Incorrectly Predicted Samples Across The Three Classes, Showing Class-Specific Performance And Misclassifications

	Predicted COVID	Predicted Normal	Predicted Pneumonia
Actual COVID	10	2	11
Actual Normal	1	39	28
Actual Pneumonia	4	13	150

Overall Accuracy: 0.77

The ANOVA statistical analysis, corroborated by the boxplots, demonstrates significant differences across the three categories—Normal, Pneumonia, and COVID-19— concerning the variables Fractal Dimension, Entropy, and Edge Density. Among the variables, Edge Density demonstrates the most pronounced variation, with COVID-19 cases presenting the lowest values, presumably attributable to diffuse opacities in the lungs of infected individuals. The ANOVA F-statistic of 326.86 and a p- value of 0.0000 validate its substantial discriminative capability. Entropy emerges as a significant characteristic, with COVID-19 pictures exhibiting greater variability and median values relative to Normal and Pneumonia cases, indicative of the anomalous intensity patterns in affected lungs. The Fractal Dimension, while exhibiting a more nuanced difference, yet demonstrates statistically significant variation (p-value = 0.0044), notably affected by outliers within the COVID group. These three parameters offer complementing insights, with Edge Density and Entropy proving particularly effective in distinguishing between the chest X-ray groups in the diagnostic model.

The performance assessment of the multiclass classifier, illustrated by the ROC curve in Fig. 4 and classification metrics shown in TABLE 1 and TABLE 2, indicates favorable diagnostic potential. The model attained an overall accuracy of 77.13, demonstrating dependable distinction among COVID-19, normal, and pneumonia cases. The Area Under the Curve (AUC) results indicate robust discriminative efficacy among classes: COVID (0.84), Normal (0.87), and Pneumonia (0.82). The Pneumonia class demonstrated the greatest F1-score (0.84), bolstered by exceptional recall (0.90), indicating the model's efficacy in accurately recognising pneumonia patients. Conversely, COVID-19 instances exhibited a diminished recall (0.43), potentially because to a restricted sample size or feature overlap with other categories. The confusion matrix indicates that certain COVID patients were inaccurately categorised as Pneumonia, underscoring the difficulty in differentiating between the two due to analogous radiographic findings. Nevertheless, the macro and weighted averages (F1-scores of 0.67 and 0.76, respectively) indicate a well balanced performance, with opportunities for enhancement through feature extension or ensemble methods.

Conclusion

This paper suggested a hybrid interpretable diagnostic complexity, texture unpredictability, and edge Overall Accuracy: 0.77 information, respectively. Statistical analysis via ANOVA validated significant disparities among the classes for each feature (p-value < 0.005). Boxplots demonstrated distinct differentiation among the categories, validating the feature selection. The features were subsequently input into a Fuzzy Inference System (FIS), facilitating categorisation via expert-like reasoning amidst ambiguity. The model attained an overall accuracy of 77.13 percent, with F1- scores of 0.84 for Pneumonia, 0.64 for Normal, and 0.53 for COVID-19. Although Normal and Pneumonia were accurately categorised, COVID-19 exhibited overlap, especially with Pneumonia, as indicated by the confusion matrix. Multiclass ROC curves demonstrated satisfactory separability, with AUCs of 0.87 for Normal, 0.84 for COVID, and 0.82 for Pneumonia. Future endeavours will entail the integration of other features such as Haralick textures, Gabor responses, and spatial patterns to enhance COVID-19 discrimination. Incorporating fuzzy clustering or neuro-fuzzy systems may augment classification efficacy. The expansion to CT scans and real-time implementation in clinical environments is also anticipated.

CONFLICT OF INTEREST

The authors declare no conflict of interest.

AUTHOR CONTRIBUTIONS

S.G wrote the manuscript. M.G., S.G., and S.C. were involved in study design and performed the experiment. All authors have gone through the manuscript and approved the final version.

REFERENCES

1. Siddiqi, R., & Javaid, S. (2024). Deep learning for pneumonia detection in chest x-ray images: A comprehensive survey. Journal of imaging, 10(8), 176.
2. Ali, Z., Khan, M. A., Hamza, A., Alzahrani, A. I., Alalwan, N., Shabaz, M., & Khan, F. (2024). A deep learning-based x-ray imaging diagnosis system for classification of tuberculosis, COVID-19, and pneumonia traits using evolutionary algorithm. International Journal of Imaging Systems and Technology, 34(1), e23014.
3. Tamal, M., Alshammari, M., Alabdullah, M., Hourani, R., Alola, H. A., & Hegazi, T. M. (2021). An integrated framework with machine learning and radiomics for accurate and rapid early diagnosis of COVID-19 from Chest X-ray. Expert systems with applications, 180, 115152.
4. Chakraborty, S., Murali, B., & Mitra, A. K. (2022). An efficient deep learning model to detect COVID-19 using chest X-ray images. International Journal of Environmental Research and Public Health, 19(4), 2013.
5. Hamal, S., Mishra, B. K., Baldock, R., Sayers, W., Adhikari, T. N., & Gibson, R. M. (2024). A comparative analysis of machine learning algorithms for detecting COVID-19 using lung X-ray images. Decision Analytics Journal, 11, 100460.
6. Arias-Londoño, J. D., Gómez-García, J. A., Moro-Velázquez, L., & Godino-Llorente, J. I. (2021). Interpretable machine learning for respiratory disease detection using multi-modal data. IEEE Access. https://ieeexplore.ieee.org/document/9293268
7. Tur, K. (2024). Multi-Modal Machine Learning Approach for COVID-19 Detection Using Biomarkers and X-Ray Imaging. Diagnostics, 14(24), 2800.
8. Mohan, G., Subashini, M. M., Balan, S., & Singh, S. (2024). A multiclass deep learning algorithm for healthy lung, Covid-19 and pneumonia disease detection from chest X-ray images. Discover Artificial Intelligence, 4(1), 20.
9. Alahmari, S. S., Altazi, B., Hwang, J., Hawkins, S., & Salem, T. (2023). Explainable AI using multimodal data fusion for respiratory diagnosis. IEEE. https://ieeexplore.ieee.org/document/9895426

10. Habib, N., & Rahman, M. M. (2021). Diagnosis of corona diseases from associated genes and X-ray images using machine learningalgorithms and deep CNN. Informatics in Medicine Unlocked, 24, 100621.
11. Iqbal, A., Usman, M., & Ahmed, Z. (2022). An efficient deep learning-based framework for tuberculosis detection using chest X- ray images. Tuberculosis, 136, 102234.
12. Singh, Y., Tripathi, N., Yadav, S., Gupta, N., Kumar, A. U., & Ramesh, J. V. N. (2024). Transfer learning and chest x-ray-based image processing and modeling to detect covid-19. In Smart Technologies in Healthcare Management (pp. 240-263). CRC Press.
13. Pal, V., Pabari, H., Indoria, S., Patel, S., Krishnan, D., & Ravi, V. (2024). Multifaceted Disease Diagnosis: Leveraging Transfer Learning with Deep Convolutional Neural Networks on Chest X- Rays for COVID-19, Pneumonia, and Tuberculosis. The Open Bioinformatics Journal, 17(1).
14. Mathesul, S., Swain, D., Satapathy, S. K., Rambhad, A., Acharya, B., Gerogiannis, V. C., & Kanavos, A. (2023). COVID-19 detection from chest X-ray images based on deep learning techniques. Algorithms, 16(10), 494.
15. Irede, E. L., Aworinde, O. R., Lekan, O. K., Amienghemhen, O. D., Okonkwo, T. P., Onivefu, A. P., & Ifijen, I. H. (2024). Medical imaging: a critical review on X-ray imaging for the detection of infection. Biomedical Materials & Devices, 1-45.
16. Xue, X., Chinnaperumal, S., Abdulsahib, G. M., Manyam, R. R., Marappan, R., Raju, S. K., & Khalaf, O. I. (2023). Design and analysis of a deep learning ensemble framework model for the detection of COVID-19 and pneumonia using large-scale CT scan and X-ray image datasets. Bioengineering, 10(3), 363.
17. Ayyachamy, S. (2022). Transfer learning framework for COVID-19 detection using chest radiographic images. In COVID-19 and Medical Imaging Analysis (pp. 135–157). IGI Global. https://doi.org/10.4018/978-8-3693-8774-0.ch008
18. Kumar, S., & Bhowmik, B. (2025). EffiCOVID-net: A highly efficient convolutional neural network for COVID-19 diagnosis using chest X-ray imaging. Methods.
19. Kibria, H. B., Hossain, M. A., Rehman, S., Alahakoon, D., & Rahman, M. A. (2024). Ensemble deep learning for robust COVID-19 classification from chest X-rays. Neurocomputing, xx, 10.1007/s00521-024-10854-3. https://doi.org/10.1007/s00521-
20. 024-10854-3
21. Liu, X., Wu, W., Lin, J. C.-W., & Liu, S. (2022). A comprehensive review of deep learning applications in COVID-19 diagnosis. Current Medicinal Chemistry, 29(33), 5713–5728. https://doi.org/10.2174/1573405618666220610093740
22. Ravichandran, R., Elangovan, N. A., Krishnan, R., Thayalan, D. K., & Ponsingh, S. (2024). Fractal dimensions in oral squamous cell carcinoma: A novel diagnostic paradigm. Oral Oncology Reports, 10, 100374.
23. Haitao, S., Ning, L., Lijun, G., Fei, G., & Cheng, L. (2011). Fractal dimension analysis of MDCT images for quantifying the morphological changes of the pulmonary artery tree in patients with pulmonary hypertension. Korean Journal of Radiology, 12(3), 289.
24. Jeon, G. (2021). Information entropy algorithms for image, video, and signal processing. Entropy, 23(8), 926.
25. Sepúlveda-Fontaine, S. A., & Amigó, J. M. (2024). Applications of entropy in data analysis and machine learning: a review. Entropy, 26(12), 1126.
26. Nautiyal, A., & Pandian, R. (2017). A Reviewal On Entropy And Peculiar Operations In Image Processing. Entropy, 1, 6.
27. Canny, J. (2009). A computational approach to edge detection. IEEE Transactions on pattern analysis and machine intelligence, (6), 679-698.
28. Amer, G. M. H., & Abushaala, A. M. (2015, March). Edge detection methods. In 2015 2nd World Symposium on Web Applications and Networking (WSWAN) (pp. 1-7). IEEE.
29. Cao, Y., Wu, D., & Duan, Y. (2020). A new image edge detection algorithm based on improved Canny. Journal of Computational Methods in Science and Engineering, 20(2), 629-642.
30. Prashant. (2021). Chest X-ray (COVID-19 & Pneumonia) [Data set]. Kaggle. https://www.kaggle.com/datasets/prashant268/chest- xray-covid19-pneumonia